

Assimilation in the upper stratosphere and mesosphere: role of radiances

Benjamin Ruston, Nancy Baker, Steve Swadley, and Karl Hoppel

*Naval Research Laboratory, Marine Meteorology Division
7 Grace Hopper, Mail Stop 2, Monterey, CA, 93943, U.S.A.
Ben.Ruston@nrlmry.navy.mil*

ABSTRACT

As operational medium-range numerical weather prediction (NWP) models move their tops into the mesosphere, observational constraints are needed. There are profiles retrieved from satellite missions such as Sounding of the Atmosphere using Broadband Emission Radiometry (SABER) and the Microwave Limb Sounder (MLS) instruments, but these data are not available within the time constraints of the operational centres. The Special Sensor Microwave Imager/Sounder (SSMIS) is a 24-channel passive microwave radiometer flown on the Defense Meteorological Satellite Program (DMSP) and has six channels near the Oxygen magnetic dipole transitions which allow for sensitivity up to 90 km. Use of these channels for data assimilation requires accounting for the Zeeman splitting of the absorption lines by the Earth's magnetic field. Further, due to narrow passbands for these channels (on the order of 1 MHz), the Doppler shifts of passband centres should also be taken into account. This study will explain the pre-processing used for the SSMIS Upper Atmospheric Sounder (UAS) data, and show results of an experiment assimilating these channels. It is shown that the addition of the SSMIS-UAS data satisfactorily constrains the analysis to match the retrievals of the SABER and MLS instruments. The work does suggest that critical to correctly predicting the mesosphere is an adequate gravity wave drag scheme and that a re-investigation of the correlation length scales of both the temperature and the winds would be appropriate when extending the NWP models to these altitudes.

1 Introduction

The current operational version of the Navy Global Environmental Model (NAVGEM), as described in [Hogan et al. \(2014\)](#), has a model top of 0.04 hPa or about 70 km above sea-level. This places the NWP model top in the mesosphere where few observational data are available in near real-time. Recent studies using satellite temperature observations to examine stratospheric sudden warmings (SSWs), such as [Manney et al. \(2008\)](#), have shown descent of mesospheric features into the stratosphere. An instrument which may be able to fill this observational void is the Special Sensor Microwave Imager/Sounder (SSMIS) a 24-channel passive microwave radiometer flown on the Defense Meteorological Satellite Program (DMSP) which contains 6 channels about the Oxygen magnetic dipole transitions and have sensitivity up to 90km. [Hoppel et al. \(2013\)](#) have evaluated these channels in a prototype NWP model which extended upwards to approximately 100 km, and shown that assimilating the SSMIS UAS channels alone has reproduced the similar benefit to that of assimilating profiles retrieved from the Sounding of the Atmosphere using Broadband Emission Radiometry (SABER) and the Microwave Limb Sounder (MLS) instruments. The ability to assimilate these data required a fast radiative transfer (RT) model which took in account estimates of the Earth's magnetic field vector and the dot product of the scene propagation vector, i.e., the angle between the antenna boresight and the vector of the Earth geomagnetic field. A fast forward model for these channels has been developed by [Han et al. \(2007, 2010\)](#) and implemented into the Community Radiative Transfer Model (CRTM) developed by National Aeronautics and Space Administration (NASA)/National Oceanic and Atmospheric Administration (NOAA)/Air Force/Navy Joint Center for

Satellite Data Assimilation. In this study we will reprise some of the key findings from the [Hoppel et al. \(2013\)](#) evaluation, and extend this to NAVGEM version 1.3 which is to be run operationally at Fleet Numerical Meteorology and Oceanography Center (FNMOC). Due to the model top of 0.04 hPa only four of the SSMIS UAS channels can effectively be assimilated. The preparation of the data will be performed by the SSMIS UAS Unified Pre-Processor (UPP) which was co-developed by the Naval Research Laboratory (NRL) and the Met Office of the United Kingdom. In addition to the assimilation of the SSMIS UAS, NAVGEM version 1.3 contains a gravity wave drag scheme which includes a stochastic parameterization for non-orographic gravity waves from [Eckermann \(2011\)](#). Comparisons will be shown between NAVGEM v1.3 both with and without SSMIS UAS assimilation. Further, passive assimilation of MLS and SABER data are performed to help independently evaluate the effect of the SSMIS UAS assimilation on the modelling system. The data used, pre-processing, and model set-up are each described in section 2. Next, section 3 will contain a brief revisit to the results from the [Hoppel et al. \(2013\)](#) study, followed by the results from the future operational NAVGEM which assimilated mesospheric data. The major findings and implications on future research are discussed and summarized in section 4.

2 Satellite Data and Model Configuration

The specific new data to be assimilated into the NAVGEM global model and data assimilation system are from the SSMIS instrument which is designed to be flown on 5 spacecraft, DMSP F-16 through F-20. A UAS specific version of the unified pre-processor (UPP) which uses the raw SSMIS temperature data records (TDRs) as input, has been implemented to account for the different sampling and scene earth location characteristics of these channels, and to contain the extra information necessary to model the Zeeman splitting of the oxygen molecules absorption lines due to the interaction of the molecule's magnetic moment with the Earth's magnetic field. Also to be mentioned are the SABER and MLS profiles which had been assimilated in the [Hoppel et al. \(2013\)](#) study, and are passively assimilated into the current one for validation.

2.1 SSMIS Upper Atmospheric Sounder (UAS)

The SSMIS UAS has six channels located near the 61 GHz Oxygen dipole transition. A unique aspect to these channels are their use of narrow passbands, on the order of 1 MHz, which make them sensitive to the Doppler shift of the upwelling scene brightness temperature. Also the magnetic dipole of the oxygen molecule will interact with the Earth's magnetic field and accurate modelling requires knowledge of the Earth's magnetic field strength and the angle between the antenna boresight and the Earth's magnetic field vector. Details of these channels can be found in [Swadley et al. \(2013\)](#) and in Table 1.

The Doppler effect on these channels is a frequency shift due to the relative motion of the instrument with respect to the scene brightness temperature. There are two terms to consider which describe this relative motion, one from the spacecraft orbit and one from the Earth rotation. The Doppler frequency shift of due to the spacecraft motion can approach 1.2 MHz which is approximately the width of the passbands used by the SSMIS UAS channels (note all channels have either dual or quadruple passbands), while the frequency shift to due to the Earth rotation is much smaller ranging from ± 10 kHz at the poles to ± 65 kHz at the Equator with the sign changing across the instrument scan, i.e., when looking towards or away from the Earth's rotation. The shift of the centre of an individual passband due to the spacecraft motion is taken into account by a combination of hardware and

software on the spacecraft itself, while the smaller shift due to Earth rotation can be accounted for by the RT model used. The effect due to the Earth’s rotation was not accounted for in this study. An example of the Doppler frequency shifts due to the spacecraft motion, Earth rotation, and their sum is shown in Figure 1. Descending orbit Doppler shifts are shown at 10° latitude increments, with the maximum Earth rotation Doppler shifts occurring at the edge of scans near the Equator.

SSMIS UAS Channel	Center Frequency (GHz)	3-db Width (MHz)	Sampling Interval (km)
19	63.283248 ±0.285271	1.35(2)	75
20	60.792668 ±0.357892	1.35(2)	75
21	60.792668 ±0.357892 ±0.002	1.3(4)	75
22	60.792668 ±0.357892 ±0.0055	2.6(4)	75
23	60.792668 ±0.357892 ±0.016	7.35(4)	75
24	60.792668 ±0.357892 ±0.050	26.4(4)	37.5

Table 1: SSMIS UAS Channel Characteristics.

Notes:

1. Sampling interval refers to along scan direction based on 833 km altitude.
2. Number of symmetric passbands is indicated by (n) next to individual 3-db width.
3. All SSMIS UAS channels are circular polarized.

The CRTM version 2.6 used in this study includes a parameterization of the Zeeman line splitting effect, which is necessary for accurately modelling channel 19 through 21. The Earth’s magnetic field strength and vector direction are given by the SSMIS UAS UPP which estimates these two parameters using the International Geomagnetic Reference Field IGRF the 11th generation [Finlay et al. \(2010\)](#). Further the SSMIS UAS UPP resamples the channels to a common footprint of 75 km. Note that SSMIS channels 22 through 24 have been operationally assimilated since 15 September 2010, at that time by NOGAPS and the Navy Atmospheric Variational Data Assimilation System – Accelerated Representer (NAVDAS-AR), and subsequently by versions of NAVGEM and NAVDAS-AR. An example of the weighting functions computed for the SSMIS UAS channels from the NRL line-by-line microwave model including Zeeman is shown in Figure 2. The 26 μT field strength is typical of an Equatorial region while the 60 μT field is typical of a polar region. All calculations used a fixed angle between the antenna boresight and the Earth field vector. The angle between the antenna boresight and the Earth’s field vector is held constant at 90°.

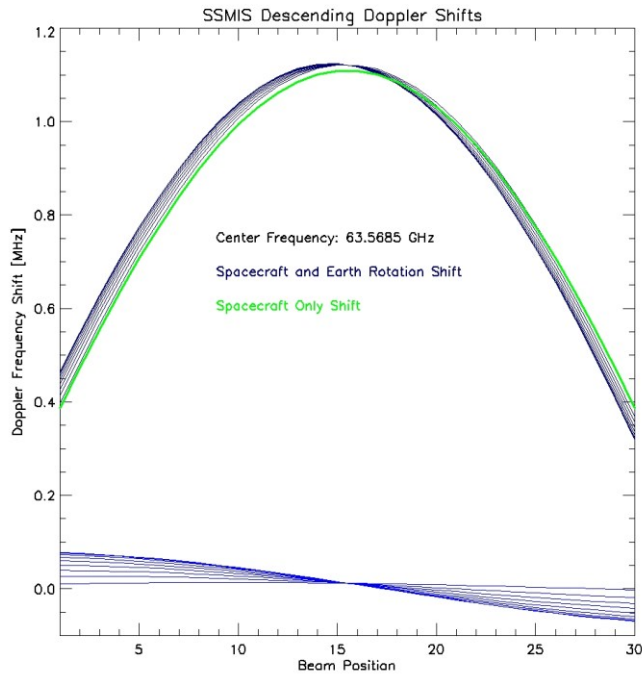


Figure 1: The Doppler frequency shift for SSMIS channel 19 on due to the spacecraft motion, Earth's rotation, and their sum. Descending orbit Doppler shifts are shown for 10° latitude increments, with the maximum Earth rotation Doppler shifts occurring at the edge of scans near the Equator.

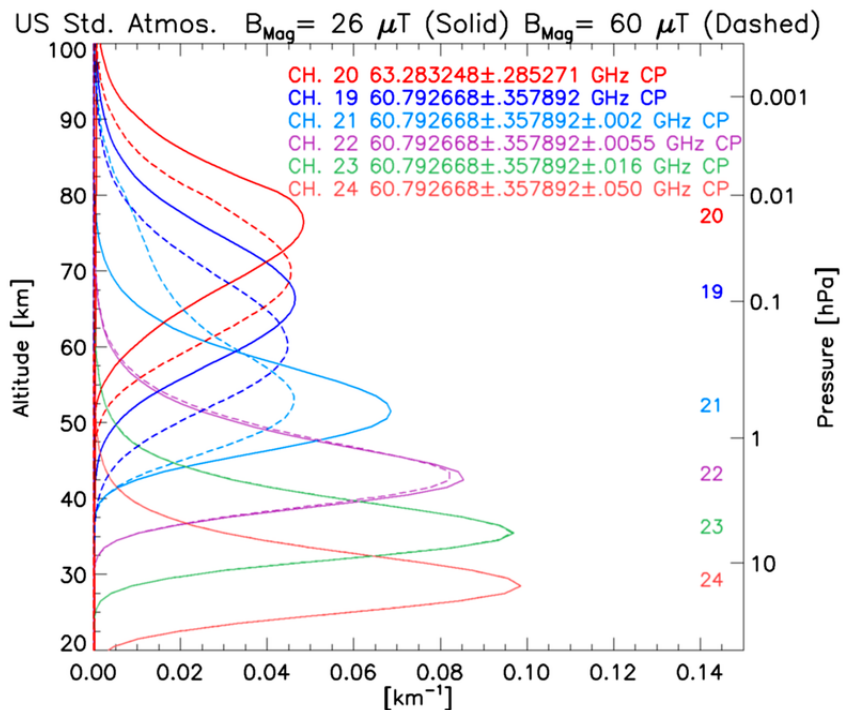


Figure 2: Shift of the weighting functions computed from the NRL line-by-line microwave model including for the SSMIS UAS channels including the Zeeman effect. The $26 \mu\text{T}$ field strength is typical of an Equatorial region, and the $60 \mu\text{T}$ field strength is typical of a polar region. The angle between the antenna boresight and the Earth's field vector is held constant at 90° .

2.2 MLS and SABER

Aboard the NASA EOS-Aura spacecraft is the Microwave Limb Sounder (MLS) instrument, for which more information can be found in [Waters et al. \(2006\)](#). This instrument has been providing global temperature and moisture profiles since July 2004 that span the upper troposphere and into the lower thermosphere. The MLS instrument retrieves atmospheric temperature using limb observation at frequencies of 118 GHz, and 234 GHz regions which each employ different Oxygen molecular lines. [Schwartz et al. \(2008\)](#) estimated precision of the temperature measurement is 1 K or better at altitudes below approximately 55 km and degrade to about 2.2 K at altitudes of 80 km. The NASA Thermosphere, Ionosphere, Mesosphere Energetics and Dynamics (TIMED) mission flies the Sounding of the Atmosphere using Broadband Emission Radiometry (SABER) instrument. The SABER instrument provides nearly continuous coverage equatorward of 52° for each hemisphere, while coverage of the higher latitudes between 52°–83° alternates every 60 days details may be found in [Remsberg et al. \(2003\)](#). [Remsberg et al. \(2008\)](#) estimated the temperature retrievals precision of 1 K at 25 km and degrading monotonically to 4 K at 80 km, they went on to report a cold bias of roughly 1 K in the upper stratosphere which grew to 2–3 K in the mid-mesosphere. In this study the MLS and SABER profiles will be used to estimate the effectiveness of the SSMIS UAS to characterize the overall mesospheric temperature structure.

2.3 NAVGEM

The U.S. Navy's high-resolution global NWP model that is run operational at the Fleet Numerical Meteorology and Oceanography Center (FNMOC) became NAVGEM in March of 2013. Details on the fundamental components of the NAVGEM prediction system can be found in [Hogan et al. \(2014\)](#). The forecast model uses both grid point and spectral (spherical harmonic) representations to perform the forecast. The NAVGEM system to be examined in this study is the pending operational release NAVGEM v1.3. NAVGEM v1.3 has a specular triangular truncation at wavenumber 425 (t425) and has 60 vertical hybrid sigma levels with the top at 0.04 hPa. A key difference, of significance for the upper stratosphere and mesosphere, between NAVGEM v1.3 and its predecessors is the inclusion of a stochastic parameterization for non-orographic gravity waves from [Eckermann \(2011\)](#). The data assimilation system included with NAVGEM, and its predecessor NOGAPS, is the 4-Dimensional data assimilation (4D-Var) system, the Navy Atmospheric Variational Data Assimilation System – Accelerated Representer (NAVDAS-AR). The current system operationally assimilates approximately 3 million observations with the key satellite sounding instruments including Infrared Atmospheric Sounder Interferometer (IASI), Advanced Microwave Sounder Unit – A (AMSU-A), Microwave Humidity Sounder (MHS), SSMIS, Atmospheric Infra-Red Sounder (AIRS), and radio occultation from receivers using the Global Navigation Satellite System (GNSS) satellite systems. The system will be augmented for this study with the SSMIS UAS radiances processed through the CRTM. The control will assimilate SSMIS channels 22–24, while the SSMIS UAS experiment will add channel 21 to the NAVGEM v1.3 configuration. SSMIS channels 19 and 20 would have a significant portion of their weighting function extend beyond the model lid, and there would be subsequent aliasing of this signal into the analysis at lower model levels.

3 Results

To begin we would like to briefly discuss the results shown by [Hoppel et al. \(2013\)](#), which importantly helped to verify the effectiveness of the CRTM to simulate the Zeeman effected channels and

secondly the ability of the SSMIS UAS to characterize the mesosphere relative to that of atmospheric profiles from MLS and SABER. To verify the effectiveness of the CRTM to simulate the Zeeman effect, [Hoppel et al. \(2013\)](#) used atmospheric profiles to simulate approximately 35,000 coincident SSMIS brightness temperature (Tb) for channel 19 both with and without the Zeeman effect included in the CRTM simulation. The atmospheric profiles are a combination of SABER profiles above 10 hPa and below this interface the NASA Goddard Earth Observing System version 5 (GEOS-5) analyses. Details on the GEOS-5 analysis have been reported by [Rienecker et al. \(2008\)](#). The results of these simulations are seen in Figure 3. They show a significant reduction in both the mean and the standard deviation of the difference between the simulation and the observed Tb, and further the variation as a function of latitude is reduced in both statistics as well.

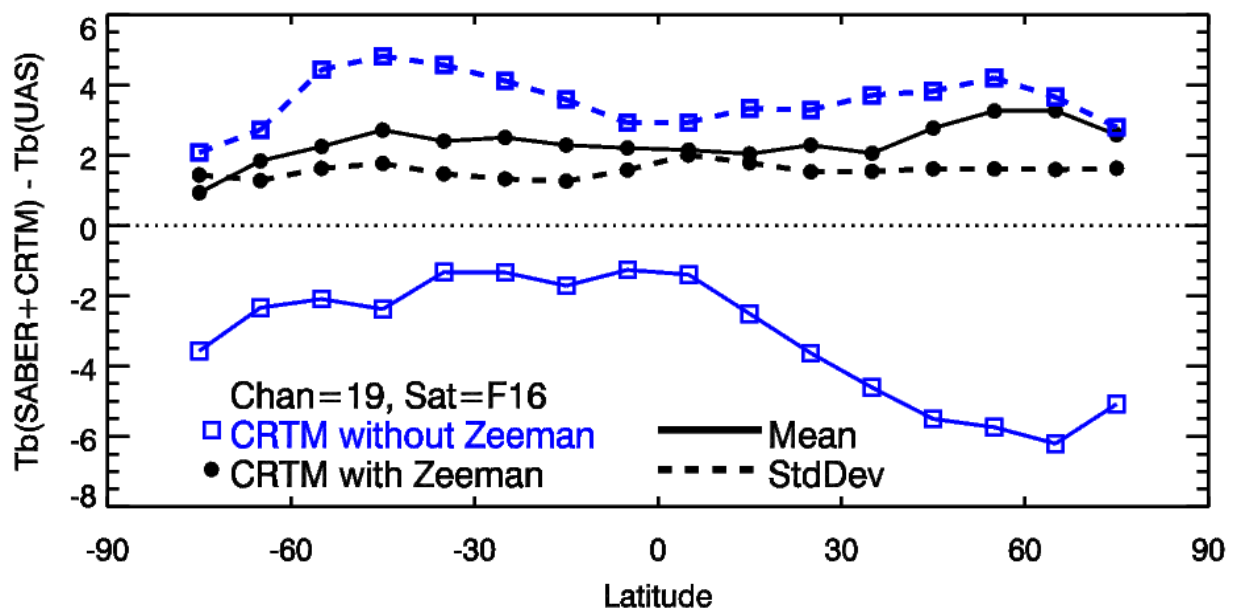


Figure 3: Mean difference (solid) and standard deviation (dashed) between approximately 35000 coincident brightness temperature from SSMIS ch19 and CRTM simulation with and without the Zeeman effect included. Data is from the 15th day of each month from April 2010 through March 2011 from a combined SABER/GEOS-5 atmospheric profile.

To verify the effectiveness of the SSMIS UAS observation to characterize the mesosphere, [Hoppel et al. \(2013\)](#) performed four experiments using a prototype NAVGEM system; this system has a spectral truncation at wavenumber 239, and 60 vertical levels with a model top of 0.005 hPa. The four experiments included: one with MLS and SABER temperature profiles, as well as SSMIS UAS channels 19–21; a second with the MLS and SABER profiles; a third with SSMIS UAS channels 19–21 alone; and a fourth with none of the MLS, SABER or SSMIS UAS data. In all experiments, MLS, SABER and SSMIS UAS data was monitored for verification purposes. The results shown in Figure 4 contain the standard deviation of the fit to the SABER profiles, the MLS profiles, and the SSMIS UAS data with the channel placed in the vertical at an average position of its weighting function for a series of cases in July of 2010. Figure 4 shows that the ability of the prototype NAVGEM system, when simulating the SSMIS UAS data alone, to effectively match the SABER and MLS profiles was similar to those experiments which assimilated these data. While the prototype NAVGEM system which didn't assimilate any of these mesospheric data, shows a substantial increase the standard deviation of the fit to each of the mesospheric data sources above 1 hPa.

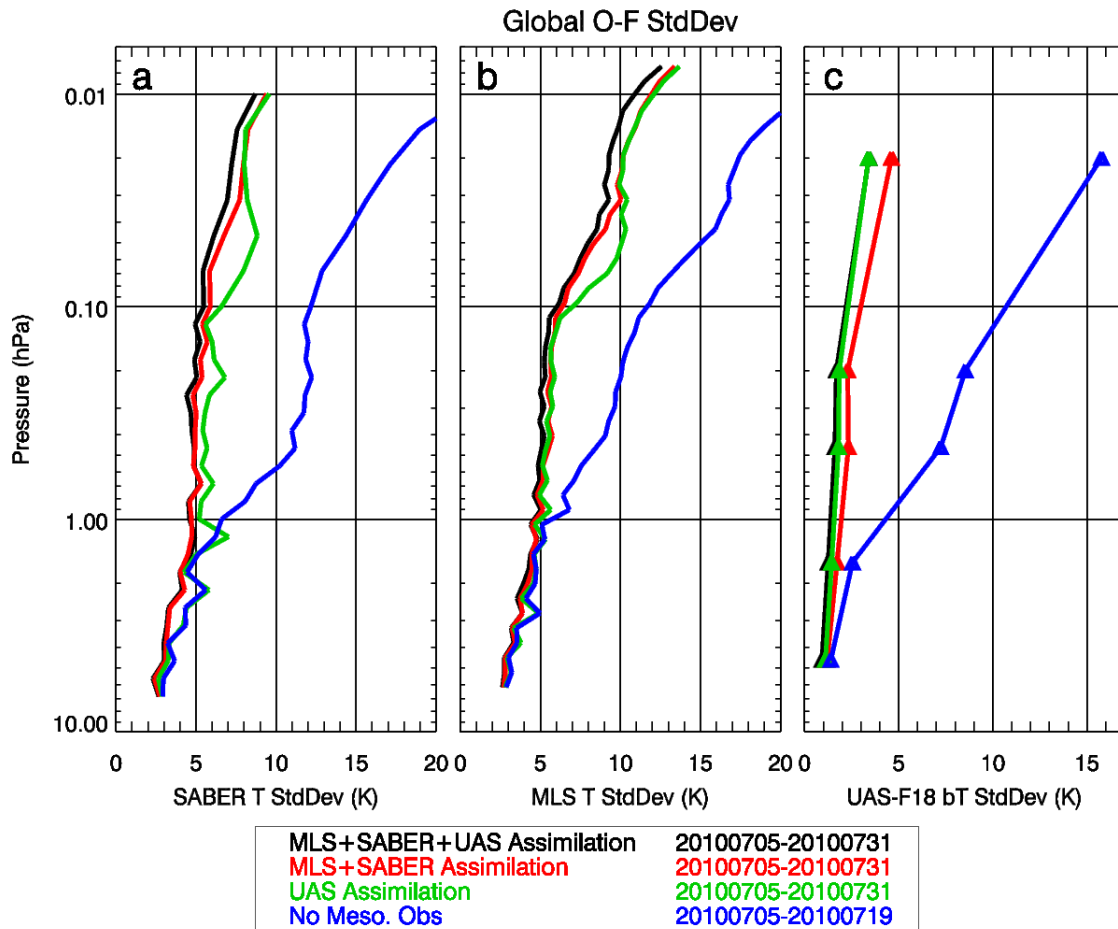


Figure 4: Standard deviation (K) of the global observed minus forecast (O-F) for (a) SABER temperatures, (b) MLS temperature, and (c) SSMIS UAS brightness temperature from DMSP F-18. Results are averaged over the period 5–31 July 2010 for all experiments except the no mesospheric observation one which was over the period 5–19 July 2010.

Next, an examination of the experiments using NAVGEM v1.3 which has a lower model lid of 0.04 hPa is undertaken. There are two experiments, a control configuration which assimilated SSMIS channels 22–24 which do not require modelling of the Zeeman effect, and a SSMIS UAS experiment which adds only channel 21. To help in independently evaluating these experiments the SABER and MLS data are passively monitored. For five update cycles from 20–21 of July 2014, the global bias between the observation from MLS and SABER and the model forecast (Observation – Forecast) are shown in Figure 5. Similarly, the global standard deviation of the difference between the MLS and SABER observation and the model forecast are shown in Figure 6. There is very little difference between the control and the SSMIS UAS experiments at pressures greater than 2.0 hPa. The bias of the model with respect to SABER and MLS then grows to about 5 K between 0.2 and 0.4 hPa; however, which experiment more closely fits the data at this level is not the same. Figure 6 does show a clear reduction in the standard deviation of the fit to the SABER and MLS data. The maximum reduction in the standard deviation of fit is approximately 3 K at 0.4 hPa. This is a much smaller reduction than was realized in the previous experiment conducted by [Hoppel et al. \(2013\)](#). It is of note that the stochastic parameterization for non-orographic gravity waves from [Eckermann \(2011\)](#) has been adjusted and implemented explicitly for the current NAVGEM v1.3 configuration. Previous

results with an earlier version of NAVGEM without the stochastic parameterization show dramatic differences in the mesospheric temperature field due to its absence.

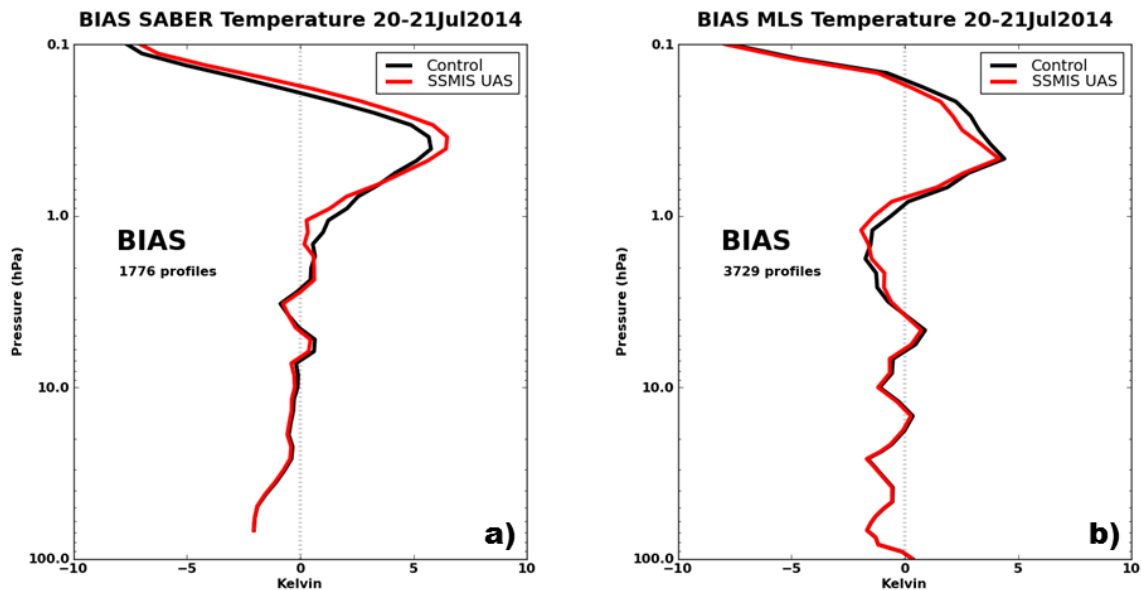


Figure 5: The global bias (K) or observed minus forecast (O-F) for (a) SABER temperatures, and (b) MLS temperature, over five update cycles from 20–21 July, 2014.

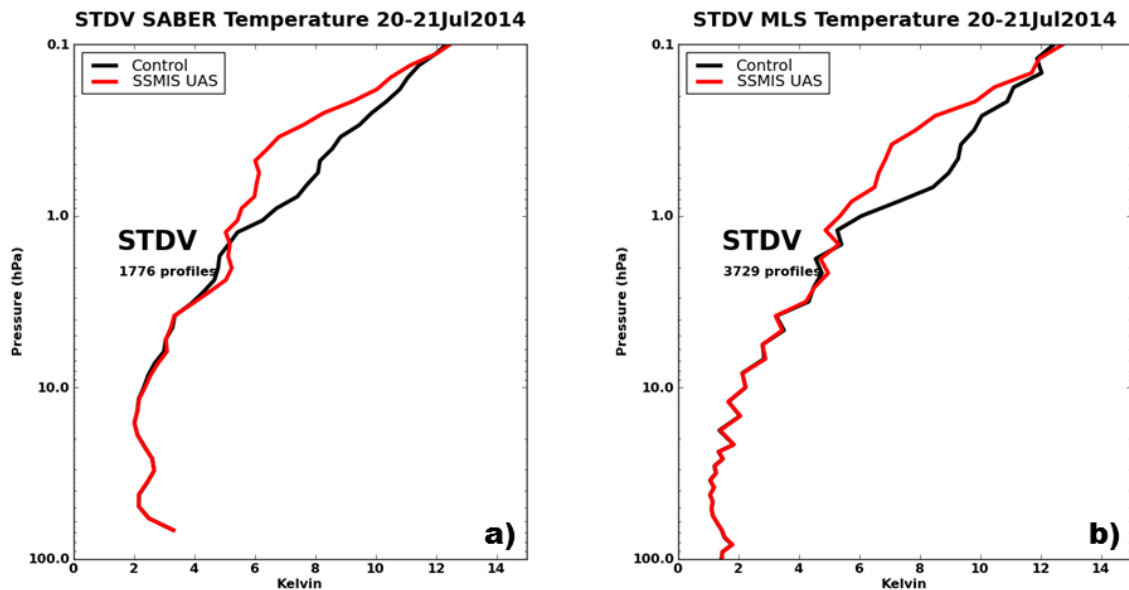


Figure 6: The global standard deviation (K) of the observed minus forecast (O-F) for (a) SABER temperatures, and (b) MLS temperature, over five update cycles from 20–21 July, 2014.

The zonal mean temperature difference between the control experiment and that including SSMIS UAS channel 21 is shown in Figure 7 on the model vertical grid for pressures less than 10 hPa. The largest effect of including SSMIS UAS channel 21 is around model level 5 which corresponds to 0.42 hPa. This is approximately the level of the peak of the channel 21 weighting function shown in Figure 2, and there is a resulting warming of the atmosphere in the high latitudes, and cooling in the northern mid-latitudes. It is important to note that this is near the stratopause, and consequentially the assimilation of this channel has an influence on its structure and placement. The atmospheric warming at the high latitudes reduces a bias relative to MLS and SABER (not shown); however, the cooling at

the mid-latitudes is sharpening the stratopause in this region which is inconsistent with these data. Further examination will be required to determine if there truly is a model bias and methodologies to correct it; in addition, a diagnosis of the specification of vertical and horizontal correlation length scales would also be appropriate.

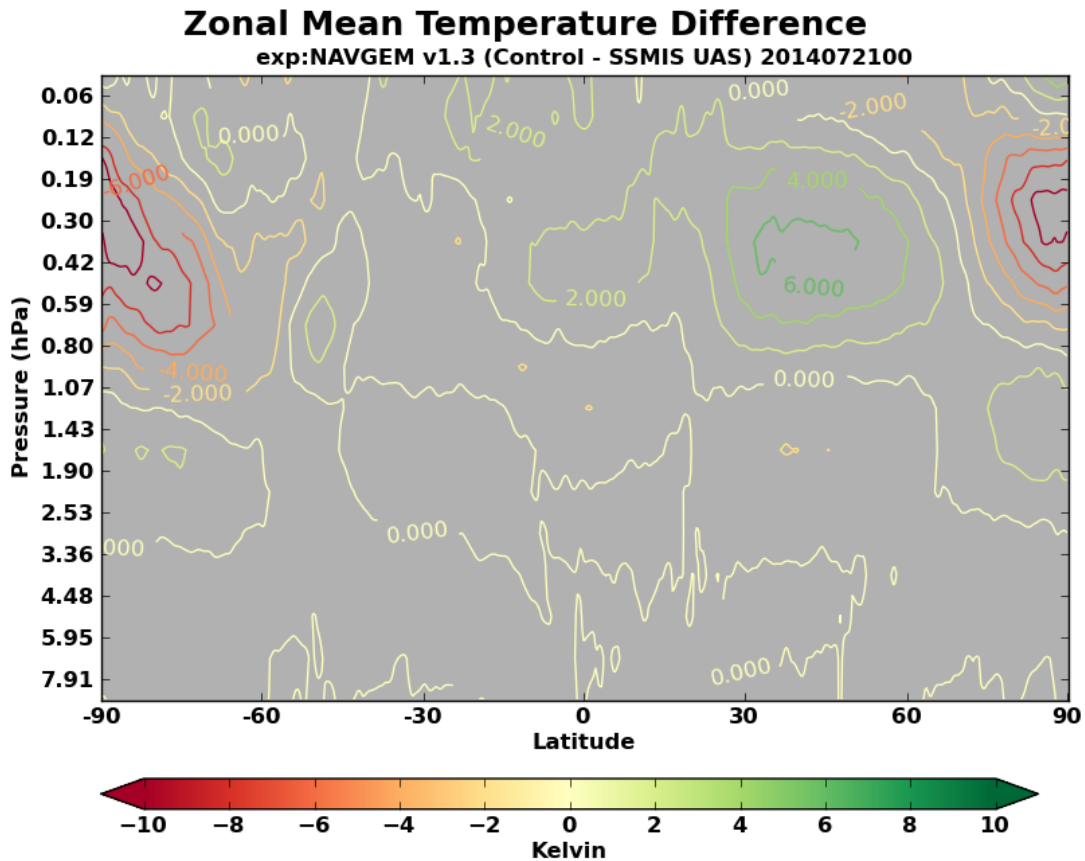


Figure 7: The zonal mean temperature difference (K) between the model analyses from the control and SSMIS UAS experiment for 21 July, 2014.

4 Summary and outlook

Use of the SSMIS UAS channels affected by Zeeman splitting of the Oxygen lines by the Earth geomagnetic field was shown. The channels require knowledge of the Earth's geomagnetic field strength and relation of the spacecraft viewing angle to the field vector. Estimates of Earth geomagnetic parameters were developed by [Finlay et al. \(2010\)](#) and released with the IGRF-11, these have subsequently been included in the SSMIS UAS Unified Pre-Processor (UPP). A fast model of the Zeeman effect was developed by [Han et al. \(2007, 2010\)](#) for the CRTM. Another consideration when using these channels is that due to the Doppler frequency shift due to the motion of the spacecraft relative to the upwelling scene brightness temperature. Because the SSMIS UAS channels all contain dual or quadruple passbands with widths on the order of 1 MHz this is of greater concern than for a typical microwave channel with a passband width on the order of 300 MHz. The frequency shift due to the Doppler effect is given by two components, one due to the spacecraft motion which is compensated for by hardware and software on the spacecraft itself and the other due to the Earth's rotation. The smaller component, due to Earth rotation, is ideally compensated for in the fast radiative transfer model by a shift of the centre frequency of the individual passbands. However, in this study

this effect was not included. Though this effect is small, an explanation of how to include this effect is discussed by Swadley et al. (2008) and will be considered for future studies.

The results of Hoppel et al. (2013) were incompletely replicated by experiments which assimilated SSMIS UAS channel 21 and used a near-operational configuration of the NAVGEM model and data assimilation system NAVDAS-AR. Though a reduction in the standard deviation of the fit to passively monitored SABER and MLS data was realized, there was a troubling bias which remained in both the control and SSMIS UAS assimilation experiment. These data show a warm bias near the top of the NAVGEM model. Inclusion of SSMIS UAS data from channel 21 did reduce regional biases relative to SABER and MLS primarily in the higher latitudes. While the impact, particularly in the northern mid-latitudes, acted to sharpen the stratopause while increasing the difference with the SABER and MLS data. Differences between the temperature analysis for the experiment and the control show an effect which can be attributed to the inclusion of the SSMIS UAS data, and the vertical placement corresponds to the weighting function peak. A re-examination of both the vertical and horizontal correlation length scales is a logical next step to find if these are appropriate for the extension of the model into the mesosphere. Further, the stochastic gravity wave drag scheme of Eckermann (2011) has substantially improved the mesospheric characterization of the NAVGEM system, even when no mesospheric data is assimilated; however, further modifications or possibly additional mesospheric layers could allow this scheme to correct biases relative to the research data available from SABER and MLS.

References

- Eckermann, J. R., 2011: Explicitly Stochastic Parameterization of Nonorographic Gravity Wave Drag, *J. Atmos. Sci.*, **68**, 1749–1765.
- Hogan, T.F., M. Liu, J.A. Ridout, M.S. Peng, T.R. Whitcomb, B.C. Ruston, C.A. Reynolds, S.D. Eckermann, J.R. Moskaitis, N.L. Baker, J.P. McCormack, K.C. Viner, J.G. McLay, M.K. Flatau, L. Xu, C. Chen and S.W. Chang, 2014: The Navy Global Environmental Model. *Oceanography*, **27**, 116–125.
- Finlay, C. C., S. Maus, C. D. Beggan, T. N. Bondar, A. Chambodut, T. A. Chernova, A. Chulliat, V. P. Golovkov, B. Hamilton, M. Hamoudi, R. Holme, G. Hulot, W. Kuang, B. Langlais, V. Lesur, F. J. Lowes, H. Luhr, S. Macmillan, M. Manda, S. McLean, C. Manoj, M. Menvielle, I. Michaelis, N. Olsen, J. Rauberg, M. Rother, T. J. Sabaka, A. Tangborn, L. Toffner-Clausen, E. Thebault, A. W. P. Thomson, I. Wardinski Z. Wei and T. I. Zvereva. 2010: International Geomagnetic Reference Field: The Eleventh Generation. *Geophys. J. Int.*, **183**, 1216–1230.
- Han, Y., F. Weng, Q. Liu and P. van Delst, 2007: A fast radiative transfer model for SSMIS upper atmosphere sounding channels. *J. Geophys. Res.*, **112** (D11121), doi:10.1029/2006JD008208.
- Han, Y., P. van Delst and F. Weng, 2010: An improved fast radiative transfer model for special sensor microwave imager/sounder upper atmosphere sounding channels. *J. Geophys. Res.*, **115** (D15109), doi:10.1029/2010JS013878.
- Hoppel, K. W., S. D. Eckermann, L. Coy, G. E. Nedoluha, D. R. Allen, S. Swadley and N. L. Baker 2013: Evaluation of SSMIS Upper Atmosphere Sounding Channels for High-Altitude Data Assimilation. *Mon. Weather Rev.*, **141**, 3314–3330.
- Manney, G. L., et al., 2008: The evolution of the stratopause during the 2006 major warming: Satellite data and assimilated meteorological analyses. *J. Geophys. Res.*, **113** (D11115), doi: 10.1029/2007JD009097.

- Remsberg, E., G. Lingenfelter, V. L. Harvey, W. Grose, J. Russell III, M. Mlynczak, L. Gordley and B. T. Marshall, 2003: On the verification of the quality of SABER temperature, geopotential height, and wind fields by comparison with Met Office assimilated analyses. *J. Geophys. Res.*, **108**, doi:10.1029/2003JD003720.
- Remsberg, E. and Coauthors, 2008: Assessment of the quality of the version 1.07 temperature-versus-pressure profiles of the middle atmosphere from TIMED/SABER. *J. Geophys. Res.*, **113**(D17101), doi:10.1029/2008JD010013.
- Rienecker, M. M. and Coauthors, 2008: The GEOS-5 data assimilation system: Documentation of versions 5.0.1, 5.1.0, and 5.2.0. *NASA Tech. Rep. 104606*, **27**, 118 pp.
- Schwartz, M. J., and Coauthors, 2008: Validation of the Aura Microwave Limb Sounder temperature and geopotential height measurements. *J. Geophys. Res.*, **113**, D15S11, doi:10.1029/2007JS008783.
- Swadley, S. D., G. A. Poe, W. Bell, Y. Hong, D. B. Kunkee, I. S. McDermid and T. Leblanc, 2008: Analysis and Characterization of the SSMIS Upper Atmosphere Sounding Channel Measurements. *IEEE Trans. Geosci. Remote Sens.*, **46**, 962–983.
- Waters, J. W. and Coauthors, 2006: The Earth Observing System Microwave Limb Sounder (EOS MLS) on the Aura satellite. *IEEE Trans. Geosci. Remote Sens.*, **44**, 1075–1092.